Biochemistry

 Volume 41, Number 33 August 20, 2002

Accelerated Publications

The Rate of Internal Heme−Heme Electron Transfer in Cytochrome *c* Oxidase†

Andreas Namslauer,‡ Magnus Brändén,‡ and Peter Brzezinski*

Department of Biochemistry and Biophysics, The Arrhenius Laboratories for Natural Sciences, Stockholm University, SE-106 91 Stockholm, Sweden

Received April 17, 2002; Revised Manuscript Received June 28, 2002

ABSTRACT: Cytochrome *c* oxidase catalyzes the one-electron oxidation of four molecules of cytochrome *c* and the four-electron reduction of dioxygen to water. The process involves a number of intramolecular electron-transfer reactions, one of which takes place between the two hemes of the enzyme, hemes *a* and a_3, with a rate of $\sim 3 \times 10^5$ s^{-1} ($\tau \cong 3$ μs). In a recent report [Verkhovsky et al. (2001) *Biochim. Biophys. Acta 1506*, 143−146], it was suggested that the 3×10^5 s^{-1} electron transfer may be controlled by structural rearrangements and that there is an additional electron transfer that is several orders of magnitude faster. In the present study, we have reinvestigated the spectral changes occurring in the nanosecond and microsecond time frames after photolysis of CO from the fully reduced and mixed-valence enzymes. On the basis of the differences between them, we conclude that in the bovine enzyme the microscopic forward and reverse rate constants for the electron-transfer reactions from heme *a* to heme a_3 are not faster than $\sim 2 \times 10^5$ and $\sim 1 \times 10^5$ s^{-1}, respectively.

Cytochrome *c* oxidase is a membrane-bound enzyme that catalyzes reduction of O_2 to water using electrons from cytochrome *c*. Initially, the electrons are transferred from cytochrome *c* to the Cu_A[1] center of cytochrome *c* oxidase, followed by consecutive electron transfer to heme *a* and to the binuclear center consisting of heme a_3 and Cu_B. When the binuclear center is reduced, oxygen binds and is reduced in a number of discrete steps.

The crystal structures of several different respiratory oxidases (*1*−*5*) have made it possible to discuss the internal electron-transfer reactions in cytochrome *c* oxidase in the context of theoretical models for electron tunneling in biological systems (*6*−*10*). An experimental method that has been used extensively to investigate electron-transfer reactions in biological systems makes use of compounds that can be attached to the protein and that eject electrons upon light excitation [for a review, see (*11*)]. However, this method cannot be used to investigate the electron transfer between

† These studies were supported by grants from The Swedish Research Council (VR), The Swedish Foundation for International Cooperation in Research and Higher Education (STINT), and the Human Frontier Science Program (HFSP).

* Corresponding author. Fax: (+46)-8-153679, Phone: (+46)-8-163280; E-mail: peterb@dbb.su.se.

‡ These authors have contributed equally to the presented work.

[1] Abbreviations: Cu_A, copper A; Cu_B, copper B; kinetic difference spectrum, the difference, of a kinetic phase, in absorbance at $t \rightarrow \infty$ minus that at $t = 0$; 2-μs phase, the kinetic phase observed after flash-induced dissociation of CO from the fully reduced enzyme; 3-μs electron transfer, electron transfer from heme a_3 to heme *a* observed after flash-induced dissociation of CO from the mixed-valence enzyme; CO-photolysis step, the unresolved absorbance change upon pulsed illumination of the enzyme−CO complex; CO-photolysis spectrum, the difference spectrum of the CO-photolysis step with either the mixed-valence ($\Delta A_{MV,CO}$) or the fully reduced ($\Delta A_{FR,CO}$) enzyme; CO-photolysis difference spectrum, the (double) difference spectrum of the CO-photolysis spectra measured with the mixed-valence and fully reduced enzymes ($\Delta A_{MV,CO} - \Delta A_{FR,CO}$); Soret region, in this study the wavelength region 400−470 nm; alpha region, in this study the wavelength region 580−630 nm; τ, time constant, 1/(rate constant); k_{ab}, k_{ba}, electron-transfer rate constants from heme *a* to heme a_3 in the forward and backward directions, respectively.

10.1021/bi025976y CCC: $22.00
Published on Web 07/25/2002

the two hemes of cytochrome *c* oxidase because electrons normally enter through Cu_A and the electron transfer from Cu_A to heme *a* is rate-limiting for the electron transfer from heme *a* to heme a_3. An alternative method that has been used extensively to investigate intramolecular electron transfer in cytochrome *c* oxidase is based on the possibility to prepare a "mixed-valence" state of the enzyme in which heme *a* and Cu_A are oxidized and the binuclear center is reduced with carbon monoxide bound to heme a_3 (*12*, *13*). In this form, the CO ligand stabilizes the reduced state of the binuclear center. Thus, flash photolysis of CO results in a lowering of the apparent midpoint potential of heme a_3, which results in equilibration of the electron with heme *a* (*14*−*18*):

$$aa_3^{-}-\mathrm{CO} \underset{k_{rec}}{\overset{k_{diss}(h\nu)}{\rightleftharpoons}} aa_3^{-} \overset{k_{ba}}{\underset{k_{ab}}{\rightleftharpoons}} a^{-}a_3 \qquad (1)$$

where $k_{diss}(h\nu)$ and k_{rec} are the light-dependent CO dissociation and recombination rate constants, respectively, and k_{ab}, k_{ba} are electron-transfer rate constants. A minus sign indicates a reduced site. Even if in this particular experiment the net electron transfer takes place in the opposite direction compared to the "normal" sequence of electron transfer in cytochrome *c* oxidase, both the forward ($k_{ab} \cong 2 \times 10^5\ s^{-1}$) and backward ($k_{ba} \cong 1 \times 10^5\ s^{-1}$) rate constants can be determined from the observed rate constant, k_{obs} (which is equal to $k_{ab} + k_{ba}$) and the extent [proportional to $k_{ba}/(k_{ab} + k_{ba})$ of the absorbance changes (*15*, *17*, *19*, and this work)]. These electron-transfer rates are pH-independent (in the range 6−10) (*14*, *19*) and do not display any solvent deuterium isotope effect (*20*), which indicates that the electron transfer on this time scale is not coupled to protonation reactions.

During enzyme turnover, the electron-transfer rate from heme *a* to heme a_3 varies depending on the state of the binuclear center and the presence of bound oxygen intermediates, but it is normally much slower than the rate observed after flash photolysis of CO from the mixed-valence enzyme ($\sim 3 \times 10^5\ s^{-1}$, see above). Recently, Verkhovsky et al. (*21*) reported that there may be an even faster electron transfer between the two hemes. This electron transfer was not resolved kinetically, and the evidence was obtained indirectly from an analysis of the extent of kinetically unresolved absorbance changes after illumination of the mixed-valence-CO complex of the bovine enzyme. In this study, we have reinvestigated the flash-induced absorbance changes in the mixed-valence and fully reduced enzymes and conclude that the rate constant of the electron transfer from heme *a* to heme a_3 is maximally $\sim 2 \times 10^5\ s^{-1}$ in the bovine enzyme.

MATERIALS AND METHODS

Enzyme Preparation. The enzyme was prepared from bovine hearts as described (*22*).

Preparation of the Mixed-Valence and Fully Reduced Enzymes. The enzyme was solubilized at a concentration of 14 μM in 0.1% dodecyl-β-D-maltoside, 130 mM KCl, 100 mM HEPES at pH 7.0, and the sample was transferred to a modified anaerobic cuvette. For measurements at −20 °C, 30% glycerol was added to the enzyme solution. The atmosphere in the cuvette was exchanged to N_2 on a vacuum line followed by addition of CO at 1 atm. Carbon monoxide reduces the enzyme by donating two electrons to each enzyme molecule after which another CO molecule binds to heme a_3 (*23*):

$$2\mathrm{CO} + \mathrm{H_2O} + \mathrm{Cu_B}^{2+}a_3^{3+} \rightarrow \mathrm{CO_2} + 2\mathrm{H}^{+} + \mathrm{Cu_B}^{+}a_3^{2+}(\mathrm{CO}) \qquad (2)$$

The enzyme form in which heme a_3/Cu_B are reduced and heme a/Cu_A are oxidized is called the mixed-valence state. The amount of CO consumed during reduction of the enzyme is the same as that of the enzyme ($\sim$14 μM); i.e., it is negligible compared to the total CO concentration ($\sim$1 mM). At the pH used in the experiments (7.0), the mixed-valence-CO complex is formed after hours of incubation at room temperature, as defined from its characteristic absorption spectrum. We monitored the absorption spectra during formation of the mixed-valence enzyme and used the sample when no further changes in absorbance were observed; i.e., the mixed-valence state was formed in essentially the entire enzyme population. Further reduction of the enzyme to form the three-electron reduced state is a much slower process and did not occur during preparation of the mixed-valence state. The reduction level of heme *a* was monitored frequently during the flash-photolysis experiments. The formation of the partly reduced forms of cytochrome *c* oxidase has also been discussed extensively in (*24*), where it was concluded that the mixed-valence state is stable and formed in almost the entire enzyme population. After investigation of the mixed-valence enzyme, the same sample was reduced using dithionite ($\sim$500 μM) or ascorbate (2 mM) and PMS (5 μM) to form the fully reduced enzyme, and the measurements were then repeated.

Kinetic Measurements. The kinetic measurements were performed using a locally modified flash-photolysis setup (LKS.60 from Applied Photophysics) described in detail in (*25*). Where applicable, the rise time of the setup was improved up to $\sim$10 ns (see figure legends). The timing of the experiment was controlled by a Digital Delay/Pulse Generator (Berkeley Nucleonics, model 555-4c). The 150-W xenon bulb providing the monitoring beam was pulsed, producing a stable light level during $\sim$500 μs. The signal was recorded using a photomultiplier (R928, Hamamatsu, 5-stage), and either it was amplified using a current-to-voltage converter (Femto, model HCA 40M-100k-C, with a bandwidth of 40 MHz and amplification of 10^5 V/A) or the output current was passed through a 50 Ω resistor and amplified using an amplifier (EG&G PARC, model 115, with a band width of 70 MHz and a rise time of 7 ns). The voltage changes were monitored using a digital oscilloscope (Hewlett-Packard, model Infinium 54820A, 500 MHz). The reaction was initiated by flash photolysis of the enzyme−CO complex using a 6-ns, $\sim$50-mJ laser flash at 532 nm (Quantel Brilliant B, Les Ulis Cedex, France).

At each wavelength, 10^4 points were collected, and the data set was then reduced to $\sim$1000 data points by averaging over a progressively increasing number of points (logarithmic time scale). Kinetic difference spectra were obtained from a global fit, with an exponential function, of kinetic traces collected at single wavelengths. The difference amplitudes at each wavelength were determined from the absorbance at $t \rightarrow \infty$ minus that extrapolated to $t = 0$. The CO-photolysis

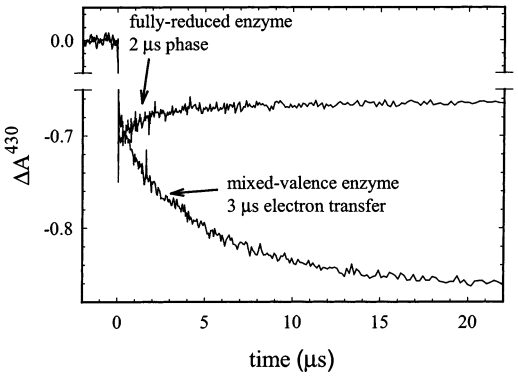

FIGURE 1: Absorbance changes at 430 nm after flash-induced dissociation of CO (at $t = 0$) from the mixed-valence and the fully reduced enzymes. The time resolution of the experimental setup was ~20 ns (bandwidth of the amplifier 40 MHz). The traces are the averages of ~30 traces and have been filtered over a number of points that increased with increasing time. Conditions: 14 μM cytochrome *c* oxidase in 0.1% dodecyl-β-D-maltoside, 130 mM KCl, 100 mM HEPES at pH 7.0, 1 mM CO, $T = +20$ °C.

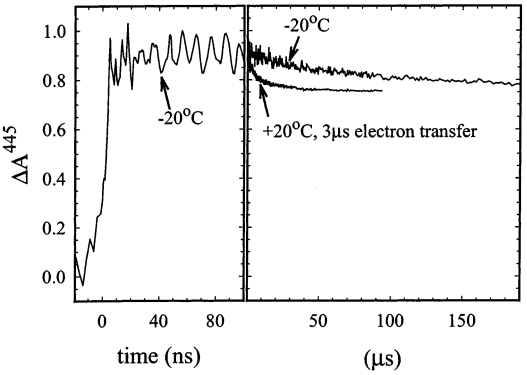

FIGURE 2: Absorbance changes after flash-induced dissociation of CO (at $t = 0$) from the mixed-valence enzyme at 445 nm at −20 °C compared to those measured at +20 °C. The bandwidth of the experimental setup was 70 MHz (the rise time 7 ns). The traces are the averages of ~20 traces, and the traces on the right-hand side have been filtered over a number of points that increased with increasing time. Conditions were the same as in Figure 1, except that the temperature was as indicated in the graph and 30% glycerol was present in the sample measured at −20 °C.

spectra (the difference spectra of the CO-photolysis steps at various wavelengths) were determined as the difference in absorbance at $t = 0$, immediately after the flash minus that before the flash.

RESULTS

Figure 1 shows absorbance changes after flash-induced dissociation of CO from the mixed-valence bovine enzyme at 430 nm (lower trace). The initial, kinetically unresolved decrease in absorbance at $t = 0$ (called "CO-photolysis step" throughout the text) is associated with dissociation of CO from heme a_3 (see also Discussion). It is followed by a further decrease in absorbance with a rate constant of 3×10^5 s^{-1} at 20 ± 1 °C ($\tau \cong 3$ μs, called "3-μs electron transfer" throughout the text), associated with net electron transfer from heme a_3 to heme *a*. This electron transfer is followed by an electron equilibration between heme *a* and Cu_A with a time constant of 30 μs, but the extent of this reaction is less than 5% in the bovine enzyme.

Figure 2 shows absorbance changes following flash-induced dissociation of CO from the mixed-valence enzyme at 445 nm and −20 °C. As seen in the figure, the absorbance increases with a time constant of ~10 ns, i.e., the time resolution of our measuring system. No significant absorbance changes were observed other than a decrease in absorbance with a rate constant of $\sim 2 \times 10^4$ s^{-1}. The $\sim 2 \times 10^4$ s^{-1} decrease is due to electron transfer from heme a_3 to heme *a*; i.e., it corresponds to the 3×10^5 s^{-1} reaction discussed above measured at +20 °C (also shown in Figure 2).

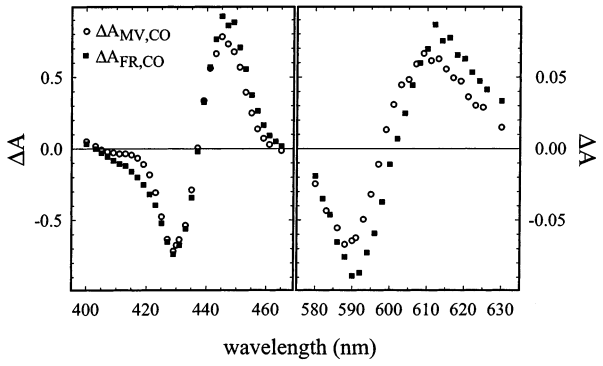

FIGURE 3: Difference spectra (CO-photolysis spectra) of the rapid, unresolved absorbance changes (CO-photolysis steps) observed upon flash-induced dissociation of CO from the mixed-valence ($\Delta A_{MV,CO}$, "○") and fully reduced ($\Delta A_{FR,CO}$, "■") enzymes. The difference spectra were determined as the absorbance difference immediately after the laser flash (with a resolution of 20 ns between measured points) minus that before the flash. Please note the different ordinate scales in the two parts of the graph. Conditions were the same as in Figure 1.

Also with the fully reduced enzyme, the initial rapid, kinetically unresolved decrease in absorbance at 430 nm is associated with dissociation of CO from heme a_3 (Figure 1). It is followed by a slower increase in absorbance at 430 nm with a rate constant of 5×10^5 s^{-1} ($\tau \cong 2$ μs, called "2-μs phase" throughout the text). This absorbance change has previously been attributed to structural rearrangements at the binuclear center associated with the release of CO from Cu_B to which it binds transiently after flash-induced dissociation from heme a_3 (*26*−*28*). With both the mixed-valence and fully reduced enzymes, CO recombines on a millisecond time scale to the original states, which makes it possible to repeat the experiment and average many traces (see figure legends). Both the 3-μs electron transfer and the 2-μs phase are seen also at other wavelengths (see below). Traces at 430 nm are shown in Figure 1 because at this wavelength the absorbance changes are relatively large and have different signs.

Figure 3 shows the CO-photolysis spectra (i.e., the difference spectra of the CO-photolysis steps) measured with the mixed-valence ($\Delta A_{MV,CO}$) and fully reduced ($\Delta A_{FR,CO}$) forms of the enzyme. These changes include only the unresolved (on a time scale of 20 ns) flash-induced changes in absorbance, before the 3-μs electron transfer in the mixed-valence enzyme or the 2-μs phase in the fully reduced enzyme. As seen in Figure 3, these initial, unresolved absorbance changes are different in the two enzyme forms.

Figure 4 shows the difference between the two spectra shown in Figure 3 (i.e., the CO-photolysis difference spectrum, $\Delta A_{MV,CO} - \Delta A_{FR,CO}$). It is displayed together with the kinetic difference spectrum of the 3-μs electron transfer measured with the mixed-valence enzyme and the kinetic

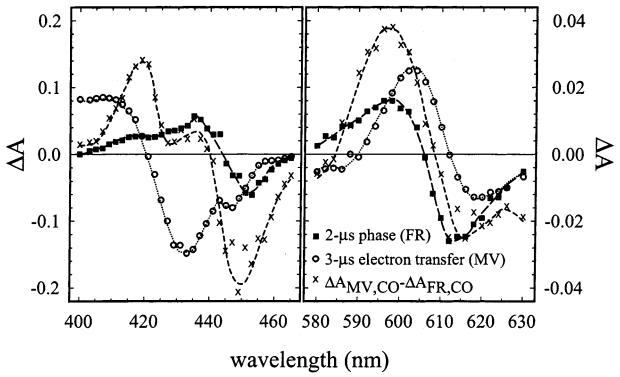

FIGURE 4: Kinetic difference spectra of the 2-μs phase measured with the fully reduced enzyme ("■") (see Figure 1), 3-μs electron transfer between heme a_3 and heme a in mixed-valence enzyme ("○") (see Figure 1), and the CO-photolysis difference spectrum, $\Delta A_{MV,CO} - \Delta A_{FR,CO}$ ("×", see Figure 3). The lines are guides for the eye. Please note the different ordinate scales in the two parts of the graph. Conditions were the same as in Figure 1.

difference spectrum of the 2-μs phase measured with the fully reduced enzyme (see Figure 1). These kinetic difference spectra were obtained from a global fit of data collected at single wavelengths.

In experiments with the fully reduced enzyme, the same results were obtained independently of whether ascorbate or dithionite was used to reduce the enzyme.

DISCUSSION

The distance between the iron ions, i.e., the centers of the hemes, is ~13 Å, while the shortest distance between the edges of the aromatic heme systems is ~7 Å (*1, 2, 5*). Therefore, when calculating the electron-transfer rate between the hemes using theoretical models, the result depends strongly on the distance used, i.e., whether the electron transfer is assumed to occur between the iron ions or the edges of the heme groups. Using one approach (*9, 10*) and a reasonable driving force, a reorganization energy, and a distance of 6.9 Å, the rate was estimated to be 7×10^8 s^{-1} (*21*). Another approach (*7*) which takes into account possible pathways between the hemes gave rates close to the measured ~10^5 s^{-1} (*29, 30*).

In this study, we have investigated absorbance changes following flash-induced dissociation of CO from the mixed-valence and fully reduced bovine cytochrome *c* oxidase. With the mixed-valence enzyme, photodissociation of CO results in absorbance changes with an observed rate constant of 3×10^5 s^{-1} ($\tau \cong 3$ μs) (*14, 18, 19*). Earlier studies [(*15*−*17, 21*), see also (*14, 19*)] have shown that the kinetic difference spectrum of the 3×10^5 s^{-1} event fits well with a static difference spectrum corresponding to electron transfer from heme a_3 to heme a, $\Delta A(a_3^{2+}a^{3+} \rightarrow a_3^{3+}a^{2+})$. Also the results from this study are consistent with the 3×10^5 s^{-1} absorbance change being associated with heme−heme electron transfer with an extent of ~30%, which is slightly larger than reported before (*15, 19*). It is not clear whether or not the events associated with the 2-μs phase (observed with the fully reduced enzyme) also take place in the mixed-valence enzyme (because the time constants are so similar). Independently of whether of not absorbance changes of the 2-μs phase are subtracted from those of the 3-μs electron transfer, it is possible to obtain a reasonable fit of the kinetic difference spectrum with static absorbance spectra corresponding to electron transfer from heme a_3 to heme a (see Supporting Information).

In a recent study by Verkhovsky et al. (*21*), the difference between the rapid, unresolved absorbance changes upon CO dissociation from the mixed-valence and fully reduced enzymes (i.e., the CO-photolysis difference spectrum) was compared to the kinetic difference spectrum of the 3-μs electron transfer in the alpha region (570−620 nm). On the basis of a similarity between these spectra, they suggested that there is an additional, "ultrafast" ($\tau < 100$ ns) electron transfer hidden in the CO-photolysis step of the mixed-valence enzyme. We also found a similarity between the kinetic difference spectrum of the 3-μs electron transfer and the CO-photolysis difference spectrum ($\Delta A_{MV,CO} - \Delta A_{FR,CO}$) in the alpha region (cf. "○" and "×" in Figure 4). However, in the Soret region (400−470 nm), these difference spectra are very dissimilar, which indicates that there is no additional internal electron transfer in the mixed-valence enzyme "hidden" within the unresolved absorbance change at $t = 0$. This conclusion is further supported by results from experiments with the *R. sphaeroides* cytochrome *c* oxidase. With this enzyme, the extent of the 3-μs electron transfer is about 3 times larger than that found with the bovine enzyme, i.e., ~90% (not shown). This means that a potential ultrafast electron transfer from heme a_3 to heme a could account for at most 10% in the *R. sphaeroides* enzyme, as compared to 35% estimated for the bovine enzyme (*21*). Different extents of ultrafast electron transfer should be manifested in different amplitudes of the CO-photolysis difference spectra. Nevertheless, these spectra were the same for the two enzymes, which indicates that the CO-photolysis difference spectrum must be due to some other process than electron transfer.

To further investigate the presence of any rapid absorbance changes after flash photolysis of CO from the mixed-valence enzyme, we did measurements at −20 °C with a time resolution of 10 ns (see Figure 2). The results indicate that there is no electron transfer from heme a_3 to heme a on this time scale. If there was an electron transfer and it had a slightly larger extent compared to that of the 3-μs electron transfer (as suggested in *21*), it would be manifested as a decrease in absorbance with a slightly larger amplitude than that of the 2×10^4 s^{-1} phase (corresponds to the 3-μs electron transfer at +20 °C, cf. Figure 2). Assuming the parameters given in (*21*), the electron-transfer rate would be about 10 times slower at −20 °C than at +20 °C. Therefore, the absence of absorbance changes in Figure 2 (where absorbance changes were measured with a time resolution of ~10 ns) indicates that at room temperature there are no electron-transfer reactions that are in the range ~1 ns−3 μs.

In addition, we also did a preliminary study of absorbance changes after flash photolysis of CO from the mixed-valence enzyme−CO complex with femtosecond time resolution (unpublished results) and could not observe any absorbance changes associated with electron transfer on a time scale 100 fs−600 ps.

As seen in Figure 4, the CO-photolysis spectra obtained with the fully reduced and mixed-valence enzymes are not identical (obtained 20 ns after the flash). As discussed above, this difference is not due to electron transfer. Even though upon flash photolysis of CO from the fully reduced enzyme no internal electron-transfer reactions can take place, absor-

bance changes have been observed after CO-photolysis (*16, 17, 27, 28, 31*). It was proposed that after dissociation from heme a_3, CO binds to Cu_B, which is followed by absorbance changes on a picosecond time scale, interpreted in terms of structural rearrangements (*27, 31*). The binding of CO to Cu_B is transient, and the ligand is released to the bulk solution with a rate constant of 4.7×10^5 s^{-1} (cf. 2-μs phase in this work). The release of CO from Cu_B gives rise to an absorbance change, proposed to be due to structural changes around heme a_3 (*17, 26*−*28*).

We observed an absorbance change with a rate of 5×10^5 s^{-1} ($\tau = 2$ μs) after flash-induced dissociation of the CO ligand from the fully reduced enzyme. A kinetic difference spectrum of the phase in both the Soret and the alpha regions is shown in Figure 4, together with the kinetic difference spectrum of the 3-μs electron transfer in the mixed-valence enzyme. As seen in the figure, these kinetic difference spectra have similar features in the alpha region, while in the Soret region the contribution of the 2-μs phase is clearly different from the kinetic difference spectrum of the 3-μs electron transfer.

As discussed above, both the picosecond absorbance changes and the 2-μs phase have been attributed to structural rearrangements around heme a_3. These changes may not necessarily take place in both the mixed-valence and fully reduced enzymes, or the absorbance contributions of the corresponding events may be different in the two enzyme forms. Such differences in the picosecond event would result in different CO-photolysis steps in the two enzyme forms.

The study of Verkhovsky et al. (*21*) was stimulated by the observation that during steady-state illumination of the mixed-valence enzyme−CO complex (or removal of CO), the fraction electron transfer from heme a_3 to heme *a* was larger than that observed during the transient reaction with a time constant of 3 μs. However, it is difficult to compare rapid, flash-induced absorbance changes on the microsecond time scale with spectral changes that occur under steady-state illumination. This is because the light-induced CO dissociation may be followed by other events, such as structural rearrangements and changes in the protonation states of groups at the binuclear center, resulting in further spectral changes. These events would not be seen in the kinetic experiments if they are slower than CO recombination. In addition, the details of the static absorbance spectra, used to calculate the difference spectrum of the electron transfer from heme a_3 to heme *a*, vary, which most likely is due to the variation in the initial states of the enzyme [(*15, 32, 33*); see also Supporting Information]. Moreover, we noticed that upon continuous illumination of the mixed-valence enzyme there was additional reduction of heme *a* during the illumination process, which also gives a larger apparent degree of electron transfer.

One complication in the comparison of the absorbance changes measured with the mixed-valence and fully reduced enzymes is that the populations of the heme a_3^{2+}−CO complexes may be different in the two samples. Since the fully reduced state is prepared by addition of a reductant to the mixed-valence sample, in this enzyme form the population of heme a_3^{2+}−CO is expected to be essentially 100%. The question therefore arises whether or not the heme a_3^{2+}−CO complex is formed at 100% also after preparation of the mixed-valence-CO state. The mixed-valence-CO complex is

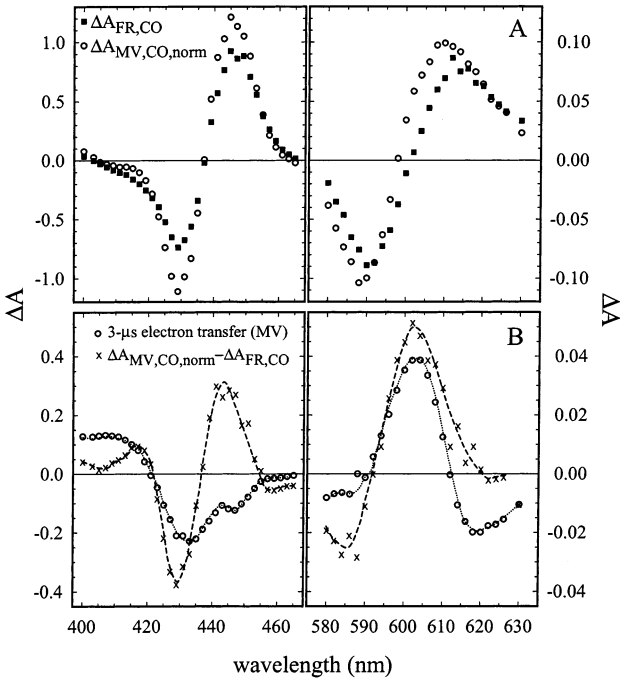

FIGURE 5: (A) The CO-photolysis spectrum measured with the mixed-valence enzyme ($\Delta A_{MV,CO,norm}$) was normalized at 592 nm to that measured with the fully reduced enzyme ($\Delta A_{FR,CO}$) (cf. Figure 3). The 592-nm wavelength is an isosbestic point for the heme a_3 to heme *a* electron transfer (see text). (B) Kinetic difference spectrum of the 3-μs electron transfer between heme a_3 and heme *a* in mixed-valence enzyme ("○") (see Figure 1) and the normalized CO-photolysis difference spectrum, $\Delta A_{MV,CO,norm} - \Delta A_{FR,CO}$ ["×", see (A)]. The lines are guides for the eye. Please note the different ordinate scales in the two parts of each graph. Conditions were the same as in Figure 1.

prepared by incubation of the oxidized enzyme under a CO atmosphere in the absence of O_2 (see Materials and Methods). Since CO is a two-electron donor, the one-electron reduced state is unlikely to be populated. The level of the three-electron reduced enzyme can easily be controlled and kept at negligible level (see Materials and Methods). Thus, the only enzyme form that may be present in addition to the mixed-valence state in the sample is the fully oxidized enzyme. As described under Materials and Methods, presumably the fraction of oxidized enzyme in the mixed-valence sample is negligible. However, below we discuss what consequences on the calculated kinetic difference spectra the presence of a fraction oxidized enzyme would have if this form was present in the mixed-valence enzyme sample.

The oxidized enzyme does not contribute to any of the absorbance changes, and therefore the only effect would be to lower the effective concentration of the reacting enzyme. If the net concentration is lower and we want to compare the CO-photolysis difference spectra measured with the fully reduced and mixed-valence enzymes, we have to rescale the mixed-valence traces and normalize them to 100% reactive enzyme. Verkhovsky et al. (*21*) suggested that the unresolved CO-photolysis step consists of only CO dissociation and heme a_3 to heme *a* electron transfer. Assuming this scenario, the amplitude of the CO-photolysis steps should be equal in size for both the mixed-valence and fully reduced enzymes at 592 nm, which is an isosbestic point for the heme−heme electron transfer. We note that after rescaling, (Figure 5A) the spectra are essentially identical to those presented previously (*21*) and that the CO-photolysis difference

spectrum in Figure 5B is similar to the kinetic difference spectrum of 3-μs electron transfer in the alpha region. However, in the Soret region, these spectra are different. In fact, there is no scaling factor between the CO-photolysis steps that would produce a CO-photolysis difference spectrum similar to that of the 3-μs electron transfer. Consequently, we cannot attribute the difference between the CO-dissociation steps measured with the mixed-valence and fully reduced enzymes to unresolved electron transfer from heme a_3 to heme *a*.

CONCLUSIONS

Our results show that there is a difference between the CO-photolysis spectra measured with the mixed-valence and fully reduced enzymes. The CO-photolysis difference spectrum is, however, not similar to the kinetic difference spectrum of the 3-μs electron transfer from heme a_3 to heme *a*. Thus, we conclude that the unresolved spectral difference does not correspond to electron transfer between hemes *a* and a_3, and the fastest electron-transfer rate from heme *a* to a_3 in cytochrome *c* oxidase is about 2×10^5 s^{-1} (forward rate constant). Even though this rate is several orders of magnitude slower than the recently estimated rate (*21*), it is still much faster than any of the catalytic reaction steps observed during turnover of the enzyme. The results do not exclude the possibility that the 2×10^5 s^{-1} rate is controlled by structural changes and/or ligand exchange at the binuclear center.

ACKNOWLEDGMENT

We thank Ida Holmgren for technical assistance.

SUPPORTING INFORMATION AVAILABLE

A figure is presented in which we show a comparison of different static difference spectra corresponding to stoichiometric electron transfer from heme a_3 to heme *a* and the kinetic difference spectrum of the 3-μs electron transfer in mixed-valence cytochrome *c* oxidase. This material is available free of charge via the Internet at http://pubs.acs.org.

REFERENCES

1. Iwata, S., Ostermeier, C., Ludwig, B., and Michel, H. (1995) *Nature 376*, 660−669.
2. Tsukihara, T., Aoyama, H., Yamashita, E., Tomizaki, T., Yamaguchi, H., Shinzawa-Itoh, K., Nakashima, R., Yaono, R., and Yoshikawa, S. (1995) *Science 269*, 1069−1074.
3. Soulimane, T., Buse, G., Bourenkov, G. P., Bartunik, H. D., Huber, R., and Than, M. E. (2000) *EMBO J. 19*, 1766−1776.
4. Abramson, J., Riistama, S., Larsson, G., Jasaitis, A., Svensson-Ek, M., Laakkonen, L., Puustinen, A., Iwata, S., and Wikström, M. (2000) *Nat. Struct. Biol. 7*, 910−917.
5. Svensson-Ek, M., Abramson, J., Larsson, G., Törnroth, S., Brzezinski, P., and Iwata, S. (2002) *J. Mol. Biol.* (in press).
6. Marcus, R. A., and Sutin, N. (1985) *Biochim. Biophys. Acta 811*, 265−322.
7. Gray, H. B., and Winkler, J. R. (1996) *Annu. Rev. Biochem. 65*, 537−561.
8. Onuchic, J. N., Beratan, D. N., Winkler, J. R., and Gray, H. B. (1992) *Annu. Rev. Biophys. Biomol. Struct. 21*, 349−377.
9. Moser, C. C., Keske, J. M., Warnacke, K., Farid, R. S., and Dutton, P. L. (1992) *Nature 355*, 796−802.
10. Page, C. C., Moser, C. C., Chen, X. X., and Dutton, P. L. (1999) *Nature 402*, 47−52.
11. Bellelli, A., Brunori, M., Brzezinski, P., and Wilson, M. T. (2001) *Methods 24*, 139−152.
12. Boelens, R., Wever, R., and Van Gelder, B. F. (1982) *Biochim. Biophys. Acta 682*, 264−272.
13. Brzezinski, P., and Malmström, B. G. (1987) *Biochim. Biophys. Acta 894*, 29−38.
14. Oliveberg, M., and Malmström, B. G. (1991) *Biochemistry 30*, 7053−7057.
15. Verkhovsky, M. I., Morgan, J. E., and Wikström, M. (1992) *Biochemistry 31*, 11860−11863.
16. Georgiadis, K. E., Jhon, N. I., and Einarsdóttir, O. (1994) *Biochemistry 33*, 9245−9256.
17. Einarsdóttir, Ó., Georgiadis, K. E., and Sucheta, A. (1995) *Biochemistry 34*, 496−508.
18. Brzezinski, P. (1996) *Biochemistry 35*, 5612−5615.
19. Ädelroth, P., Brzezinski, P., and Malmström, B. G. (1995) *Biochemistry 34*, 2844−2849.
20. Karpefors, M., Ädelroth, P., Aagaard, A., Smirnova, I. A., and Brzezinski, P. (1999) *Isr. J. Chem. 39*, 427−437.
21. Verkhovsky, M. I., Jasaitis, A., and Wikström, M. (2001) *Biochim. Biophys. Acta 1506*, 143−146.
22. Brandt, U., Schägger, H., and von Jagow, G. (1989) *Eur. J. Biochem. 182*, 705−711.
23. Brzezinski, P., and Malmström, B. G. (1985) *FEBS Lett. 187*, 111−114.
24. Jasaitis, A., Verkhovsky, M. I., Morgan, J. E., Verkhovskaya, M. L., and Wikström, M. (1999) *Biochemistry 38*, 2697−2706.
25. Brändén, M., Sigurdson, H., Namslauer, A., Gennis, R. B., Ädelroth, P., and Brzezinski, P. (2001) *Proc. Natl. Acad. Sci. U.S.A. 98*, 5013−5018.
26. Dyer, R. B., Einarsdóttir, Ó., Killough, P. M., Lopez-Garriga, J. J., and Woodruff, W. H. (1989) *J. Am. Chem. Soc. 111*, 7657−7659.
27. Woodruff, W. H., Einarsdóttir, Ó., Dyer, R. B., Bagley, K. A., Palmer, G., Atherton, S. J., Goldbeck, R. A., Dawes, T. D., and Kliger, D. S. (1991) *Proc. Natl. Acad. Sci. U.S.A. 88*, 2588−2592.
28. Einarsdóttir, Ó., Dyer, R. B., Lemon, D. D., Killough, P. M., Hubig, S. M., Atherton, S. J., Lopez-Garriga, J. J., Palmer, G., and Woodruff, W. H. (1993) *Biochemistry 32*, 12013−12024.
29. Regan, J. J., Ramirez, B. E., Winkler, J. R., Gray, H. B., and Malmström, B. G. (1998) *J. Bioenerg. Biomembr. 30*, 35−39.
30. Medvedev, D. M., Daizadeh, I., and Stuchebrukhov, A. A. (2000) *J. Am. Chem. Soc. 122*, 6571−6582.
31. Stoutland, P. O., Lambry, J. C., Martin, J. L., and Woodruff, W. H. (1991) *J. Phys. Chem. 95*, 6406−6408.
32. Liao, G. L., and Palmer, G. (1996) *Biochim. Biophys. Acta 1274*, 109−111.
33. Vanneste, W. H. (1966) *Biochemistry 5*, 838−848.

BI025976Y